

PAPER • OPEN ACCESS

Nozzle design influence on the steam-driven ejector

To cite this article: D V Brezgin and K E Aronson 2020 *J. Phys.: Conf. Ser.* **1683** 042013

View the [article online](#) for updates and enhancements.

<div data-bbox="130 1744 233 1814"></div> <div data-bbox="237 1751 619 1834"><p>The Electrochemical Society Advancing solid state & electrochemical science & technology 2021 Virtual Education</p></div> <div data-bbox="237 1852 769 2009"><p>Fundamentals of Electrochemistry: Basic Theory and Kinetic Methods Instructed by: Dr. James Noël Sun, Sept 19 & Mon, Sept 20 at 12h–15h ET</p></div> <div data-bbox="237 2033 555 2076"><p>Register early and save!</p></div>	
--	--

Nozzle design influence on the steam-driven ejector

D V Brezgin¹ and K E Aronson¹

¹ Ural Federal University named after first President of Russia B.N. Yeltsyn,
Russia, 620002 Ekaterinburg, Mira, 19

dvbrezgin@urfu.ru

Abstract. In the present paper, a series of numerical simulations of wet steam flows within ejectors distinguished by four primary nozzle contours have been carried out with the objective to evaluate the overall ejector performance. The studied primary nozzle contours are the following: a standard Laval nozzle (LAVAL); a nozzle that is designed in order to provide Constant Expansion Rate (CER); and two nozzles (MOC_SHORT, MOC_LONG) that are designed by employing axisymmetric Method of Characteristics. At first, the wet steam flow simulation throughout solely nozzles are carried out. Within the CFD simulations routines most valuable flow parameters are compared: expansion rates, boundary layer displacement and momentum thicknesses; entropy generation rate from various thermodynamic forces; thrust and liquid mass fraction across the nozzle exit plane. A comprehensive analysis of solely nozzles revealed that the CER nozzle contour is the most aerodynamically efficient design, which provides the minimum liquid mass fraction by the nozzle exit and possess the minimum entropy generation rate. The CFD results analysis of a full ejector domain revealed that an ejector with a MOC_SHORT primary nozzle contour provides the maximum performance in terms of secondary mass flow rate. At that, the secondary mass flow rate in MOC_SHORT nozzle contour case is almost 4% greater than for the CER nozzle design case.

1. Introduction

Steam ejectors are widely used in metallurgy, oil and gas industry, etc. On power plants, steam ejectors are used to utilize non-condensable gases from low-pressure parts of steam turbines. With the obvious simplicity of the ejector design, the flowfield features are characterized by non-trivial interaction of complex physical phenomena that occur in multiphase supersonic jets: condensation shocks, the interaction of oblique shock waves and expansion/compression waves, the development of a free shear turbulent layer, separation of the boundary layer due to the adverse pressure gradient etc. As with any jet pump, the main device component of the ejector is the primary nozzle, in which the potential energy of the vapor (pressure) is converted into kinetic energy of the jet (momentum). In this case, the supersonic primary flow involves a static secondary flow through a turbulent interaction in the free shear layer in the ejector's mixing chamber. The bulk momentum of the mixed flows determines the backpressure upper limit value, which the steam ejector is able to overcome without loss in performance. In recent years, an interest in the numerical modeling of ejectors including wet steam fluid [1, 2] is greatly increased. However, there are very few experimental studies in this area. An exception is Ref. [3], where comprehensive data are given both on the geometry of the experimental ejector and on the operating modes studied (initial steam parameters, mass flow rates of the motive and suction flows, distribution of static pressure along the wall of the mixing chamber and diffuser). Unfortunately, in Ref. [3] author does not take into account the condensation that is the flow feature of all devices with water vapour as a fluid.



In steam ejectors, namely in primary nozzles, at high degrees of the flow expansion steam supercooling always takes place. This is followed by spontaneous condensation of part of the steam and the subsequent latent heat release. As a result, additional uncertainty arises related to the influence of this complex and not yet fully studied physical phenomenon both on the thermo/fluid dynamic parameters of the motive flow (Mach number etc.) and on the turbulence parameters of a supersonic viscous flow of a real two-phase mixture. For example, in Ref. [4] the results of an international project are presented with the purpose to review the ability of computational methods to predict condensing steam flows. In this work, 13 teams, using various in-house or commercial CFD solvers, simulated the flow of wet steam in several nozzles, and then the obtained results are compared with the available experimental data (static pressure profiles and droplet diameters).

One of the conclusions in this paper is the fact that today there is no universal condensation model that could be used without verification with experiment in the entire range of initial parameters of water vapor and in all ranges of Knudsen numbers. The current situation in this field of research is complicated by the fact that often the identical condensation models (nucleation and droplet growth) but distinguished solution schemes yields in various results.

As a rule, from the manufacture simplicity point of view, supersonic profiles of steam ejectors primary nozzle represents a diverging cone with a constant expansion angle of 8-14 degrees (Laval nozzle). Such nozzle contour is employed in Ref. [3]. In aerospace engineering design tasks it has long been known that such nozzles have a number of drawbacks relative to "curved" nozzles: reduced thrust due to the presence of a radial velocity component, boundary layer separation at high degree of over-expansion of the flow. Moreover, with high degrees of expansion, the length of the nozzle may exceed the permissible mass-size characteristics and this imposes additional requirements on the nozzle designs [5]. However, it is not quite simple to make a conclusion which nozzle contour is preferable to utilize in steam ejectors because the performance of all jet pumps determined as the Entrainment Ratio Er (the secondary to the primary mass flow rates ratio) depends not so much on the flow parameters at the nozzle exit. It mainly depends on the efficiency of the momentum exchange of two streams in a free shear layer, which determines the overall ejector performance.

In this regard, the purpose of the present work is to determine the optimal contour of the primary nozzle from the standpoint of evaluating the overall steam ejector performance.

2. Numerical model

The numerical solution implemented in this work is based on a modified Eulerian Multiphase Mixture model within a widely used CFD commercial solver Ansys Fluent and the general approach employed herein described in details in Ref. [6]. The compressible form of conservation equations for continuity, momentum, total energy, liquid volume fraction ' α_l ' and number of droplets per unit of mass n can be written as,

$$\begin{aligned} \frac{\partial \rho_m}{\partial t} + \frac{\partial \rho_m u_j}{\partial x_j} &= 0 \\ \frac{\partial \rho_m u_i}{\partial t} + \frac{\partial \rho_m u_i u_j}{\partial x_j} &= -\frac{\partial p}{\partial x_j} + \frac{\partial \tau_{ij}}{\partial x_j} \\ \frac{\partial \alpha_l \rho_l E_l + \alpha_v \rho_v E_v}{\partial t} + \frac{\partial u_j [\alpha_l (\rho_l E_l + p) + \alpha_v (\rho_v E_v + p)]}{\partial x_j} &= k_{\text{eff}} \frac{\partial^2 T}{\partial x_j^2} + \frac{\partial u_i \tau_{ij}}{\partial x_j} \\ \frac{\partial \rho_l \alpha_l}{\partial t} + \frac{\partial \rho_l \alpha_l u_j}{\partial x_j} &= \alpha_v \frac{4}{3} \pi \rho_l r^{*3} J + \rho_m 4 \pi \rho_l r^2 n \frac{dr}{dt} \\ \frac{\partial \rho_m n}{\partial t} + \frac{\partial \rho_m n u_j}{\partial x_j} &= \alpha_v J \end{aligned} \quad (1)$$

, where J is the nucleation rate per unit volume of vapor per unit time, r^* is the critical radius of a stable liquid droplet and r is the radius of a generic liquid droplet. The nucleation rate is determined here through the Classical Nucleation Theory modified with Kantrowitz non-isothermal correction, whilst the droplet growth law $\left(\frac{dr}{dt}\right)$ proposed by Gyarmathy correction (more details can be found in Ref. [4]) is selected for the present work.

For the present work, IAPWS-IF97 supplementary equation of state for a part of metastable-vapor region is utilized. The thermodynamic properties of condensate in super-cooled conditions required for the calculation of phase change mechanisms are determined using several empirical relations reported in

literature. The liquid density, latent heat, surface tension and condensation coefficient are taken from the work in Ref. [7].

A Generalized $k-\omega$ (GEKO) two-equation turbulence model with $C_{sep} = 2.5$ is used to account the turbulent characteristics of the two-phase flows within all CFD tasks. The general formulation of GEKO turbulence model and its main advantages relative to more common standard $k-\omega$ or $SST\ k-\omega$ is presented in Ref. [8]. It's well-known that conventional models like $k-\omega$ or SST will over-predict spreading rates of round jets substantially while giving reasonable results for plane jets. More details about 'round-jet plane-jet' anomaly is given in Ref. [9]. However, the major reason of using such state-of-art turbulence model in present work is the model's ability to adjust sensitivity to adverse pressure gradients and spreading rates even by a non-expert by changing of free coefficients values from the given set. This feature is tremendously important while modeling ejector's flowfield because of presence of boundary layer separation and mixing layers as well.

In accordance with CFD-solver guide, a pressure-velocity coupled scheme within the pressure-based solver is selected for present work, whilst evaluation of gradients is solved with Least Squares Cell Based algorithm and PRESTO! scheme is used for interpolating the pressure values at the faces. Second order upwind scheme is used for spatial discretization of all transport equations. Pressure boundary conditions are assumed at both inlet and outlet boundaries. Walls of the nozzles are assumed as adiabatic. All the simulations conducted in the present study are 2D-axisymmetric and all the simulation domains has been discretized with well-refined structural mesh with accurate boundary layer resolution: $wall\ Y^+$ value lower than unity and at least 25 cell layers fitted within boundary layer edge.

In order to get deep insight into wet steam flowfield in terms of effectiveness of expansion work a detailed analysis is carried out for all nozzle designs. While for the boundary layer study, the additional user-defined function (UDF) that is fired on-demand has been implemented to calculate the boundary layer displacement δ and momentum θ thickness along the walls, in the freestream the nonequilibrium thermodynamic methods have been used. Particularly, the additional user-defined scalar (UDS) equation in a conventional CFD solver routine has been incorporated. Equation (2) represents the specific entropy conservation equation that has been utilized and solved as additional scalar equation alongside with the set of governing equations (1).

$$\left\{ \begin{aligned} \frac{\partial \rho_m s}{\partial t} + \frac{\partial \rho_m s u_j}{\partial x_j} &= \frac{k_{eff}}{T^2} \left(\frac{\partial T^2}{\partial x_i} + \frac{\partial T^2}{\partial x_j} \right) + \frac{\Phi + \rho_m \epsilon}{T} + \Gamma h_{lv} \left(\frac{1}{T} - \frac{1}{T_d} \right) \\ \Phi &= \mu \left(2 \left[\frac{\partial u_i^2}{\partial x_i} + \frac{\partial u_j^2}{\partial x_j} + \frac{u_j^2}{x_j} \right] + \left[\frac{\partial u_i}{\partial x_j} + \frac{\partial u_j}{\partial x_i} \right]^2 \right) - \frac{2}{3} \mu (\nabla \cdot \vec{V})^2 \end{aligned} \right. \quad (2)$$

, where s is the specific entropy, k_{eff} is the effective thermal conductivity, Φ is the dissipation function according to compressible axisymmetric formulation, ϵ is the turbulent dissipation rate, Γ is the liquid mass generation rate and h_{lv} is the latent heat. It's worth to emphasize that three source terms on RHS of the UDS (2) are related to distinct entropy generation rate sources. The first one is the entropy generation due to heat transfer; the second term is concerned to the entropy production due to viscous dissipation from the mean and fluctuating velocity gradients and the latter term is the entropy generation due to mass transfer (condensation). The general details in derivation of source terms for the entropy production rate can be found in Ref. [10].

3. Results and discussion

Forasmuch the objective of the present work is to evaluate nozzles contour in terms of steam ejector performance, the mandatory part of the study is to accomplish proper validation of the proposed numerical treatment of the entire ejector's domain against experimental data. In accordance with experimental data in Ref. [3], the proposed numerical approach is validated initially by modeling the flowfield with the default (Laval) primary nozzle contour. The CFD results have been compared with experimental ones in terms of the primary/secondary mass flow rates as well as static pressure distribution along the mixing chamber and diffuser walls. The relative errors concerned to the

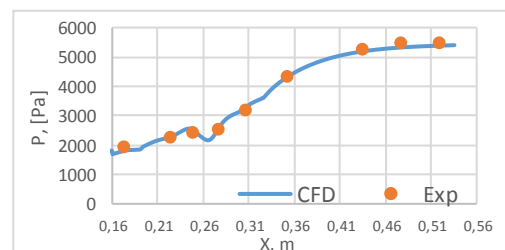


Figure 1. Comparison of experimental and numerical wall pressure profiles

appropriate mass flow rates did not exceed 5% while the static pressure assessment is performed qualitatively and the result is presented on Figure 1. By making sure that proposed numerical modeling is reasonable fitted against experimental data, it's decided to start further analysis by accomplishing CFD simulations of solely nozzles distinguished in various nozzle contours but possessing identical expansion level (the same exit diameter). Fig. 2 represents all studied nozzle contours.

For further analysis, it is necessary to describe briefly the methods for designing the nozzle contours. The LAVAL nozzle contour is a standard nozzle used in Ref. [3] in which the supersonic section represents a divergent cone with a constant expansion angle. The CER nozzle contour is designed with a Constant Expansion Rate condition and detailed explanation of the CER design method is presented in Appendix in Ref. [11]. The supersonic sections of the MOC_LONG and MOC_SHORT nozzle contours are designed by means of the Method of Characteristics in axisymmetric formulation but differs with a radius of the arc circumscribing the expansion section. Respectively, the MOC_SHORT nozzle contour distinguished by steeper rise of the flow passage and a smaller total length of the supersonic section.

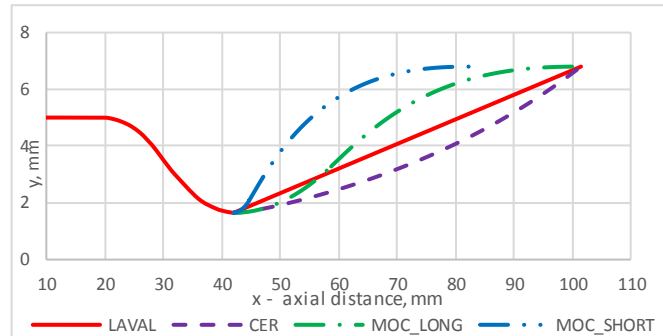


Figure 2. Nozzle profiles

The supersonic sections of the MOC_LONG and MOC_SHORT nozzle contours are designed by means of the Method of Characteristics in axisymmetric formulation but differs with a radius of the arc circumscribing the expansion section. Respectively, the MOC_SHORT nozzle contour distinguished by steeper rise of the flow passage and a smaller total length of the supersonic section.

Numerical simulations of four nozzle designs with advanced post-process study revealed major gas-dynamic features in terms of wet steam flow expansion through supersonic nozzles. Figure 3 shows normalized static pressure distribution (a) and liquid mass fraction (b) along the axis. It's evident that wall contour has significant impact on nucleation onset and subsequent droplet growth. MOC_SHORT and CER nozzles distinguish from the others in comparatively small amplitude of the condensation shock (MOC_SHORT) and gentler rise of liquid mass fraction (CER). Following to aerospace engineering best practices, it is more preferable to make nozzle comparison by evaluating area-weighted average values of most justified flow properties by the nozzle exit. It's turned out that liquid mass fraction in CER nozzle at the exit plane is less on 15% regarding to MOC_SHORT nozzle (0.149 and 0.162 accordingly). Following to Ref. [11], liquid mass fraction rate is mostly governed by the expansion rate of the particular nozzle and the post-process analysis in the present work yields that volume weighted average of the flow expansion rate of the CER nozzle is in 2.7 times less than the expansion rate of the MOC_SHORT nozzle design. This fact correlates with the following observation as well: CER nozzle distinguishes the minimum static pressure and maximum axial velocity at the nozzle exit plane by evaluating area-weighted average values. Literally, it means that CER contour has evident advantage in terms of isentropic efficiency of nozzles.

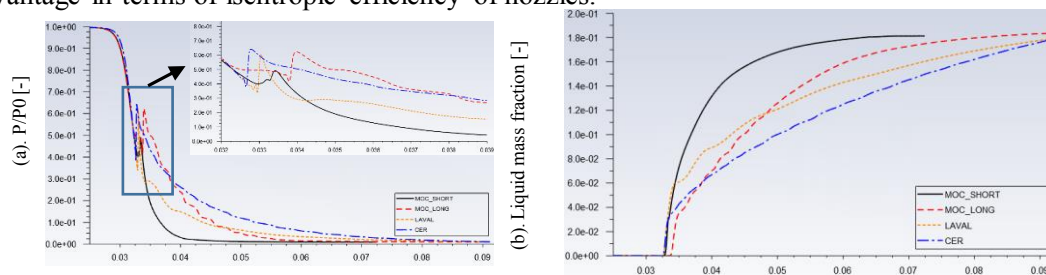


Figure 3. Normalized static pressure distribution (a) and liquid mass fraction (b) along the axis

In order to get more insight in terms of the nozzle contour efficiency the detailed analysis of the boundary layer properties and entropy generation rate within the core of the flowfield are carried out. Figure 4 shows comparison of the boundary layer displacement δ and momentum θ thickness along the wall of all the nozzle designs from the geometrical throat. It's evident that MOC_SHORT nozzle contour possess the smallest mass and momentum deficit due to the shortest length while the CER nozzle slightly overpredicts the boundary layer momentum thickness regarding to the nozzles of the same length. However, the total difference of momentum thickness between the CER and MOC_SHORT contour

reaches about 40% and such a generous deviation may potentially led to the efficiency loss in terms of ejector performance for the CER nozzle case.

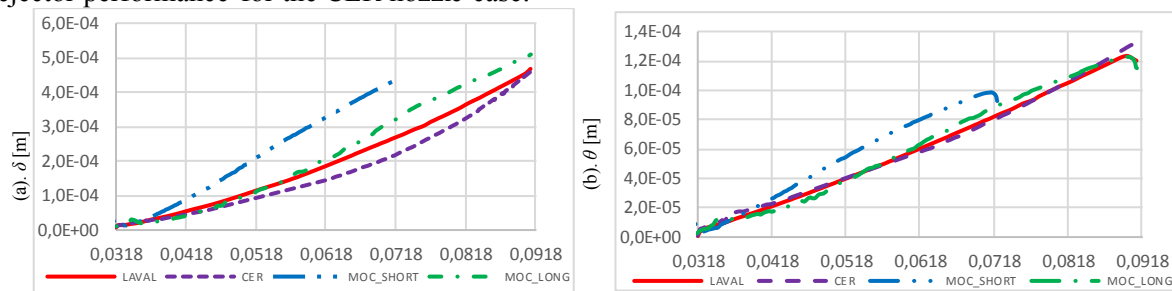


Figure 4. Boundary layer (a) displacement δ and (b) momentum θ thickness along the wall

The nonequilibrium thermodynamic analysis reveals that CER nozzle is distinguished from the others by the minimum bulk entropy generation rate (Fig. 5). It's worth to mention that the most contribution to the entropy generation rate is stemmed from the mass transfer (phase change), whilst the entropy generation due to the heat transfer have negligible impact to the net entropy gain.

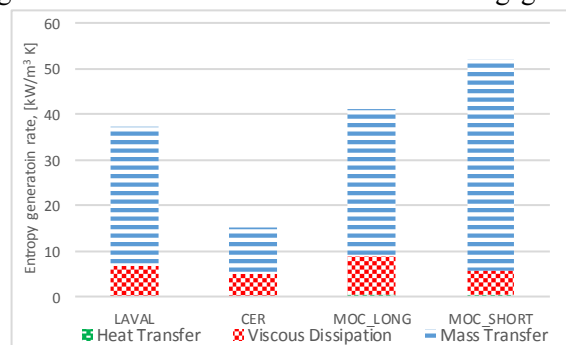


Figure 5. Entropy generation rate

Whereas CER nozzle contour justified the best aerodynamic efficiency in terms of entropy generation rate and area-weighted average values of static pressure and axial velocity at the nozzle exit plane, the thrust across the nozzle exit plane had its maximum in case of MOC_SHORT nozzle contour (about 0.6% higher than for the CER nozzle design). The thrust as a sum of the pressure forces and momentum flux is calculated by integrating the equation (3) at the nozzle exit plane in radial direction, at that actual integrating is performed by implementing Simpson's numerical

method within additional UDF fired on-demand.

$$F = 2\pi \int_0^r [(p_e - p_{amb}) + \rho u^2] r dr \quad (3)$$

The next part of the study is concerned to numerical simulations of the entire ejector's domain. As above mentioned, the proposed numerical modeling is reasonable fitted against experimental data with the default LAVAL primary nozzle contour. Therefore, additional ejector simulations with CER and two MOC primary nozzle contours have been carried out by using the same CFD treatment. Simulation results comparison revealed that ejector with MOC_SHORT primary nozzle contour provides the best performance whereas ejector with CER nozzle contour possess the worst performance. Ejector with MOC_SHORT nozzle reaches 1.9% gain in terms of secondary mass flow rates relatively to default LAVAL nozzle design whereas ejector with CER nozzle contour distinguishes in performance loss about 1.8%. Such a result appears to contradict the single nozzle CFD modeling results where the CER nozzle contour had apparent advantages among other designs except boundary layer momentum thickness. Table 1 shows the secondary mass flow rates for distinct ejector modeling cases and relative to default LAVAL nozzle mass flow rate deviation.

Table 1. Secondary mass flow rates and deviations relative to LAVAL nozzle CFD case

	LAVAL	CER	MOC SHORT	MOC LONG
Mass flow rate, kg/s	1.243e-3	1.220e-3	1.266e-3	1.247e-3
Relative to LAVAL case deviation, %	0	-1.82	+1.90	+0.39

It's noticeable that nozzle contour designed in accordance with axisymmetric method of characteristic but differs a longer expansion section (MOC_LONG) is also preferable in terms of ejector performance although the net gain is comparatively small. It should be emphasized that area-weighted average of

liquid mass fraction at the nozzle exit plane for the MOC_SHORT primary nozzle contour exceeded on almost 7% the same property for the CER case.

It is well known from the mixing layer theory that turbulence is the only transport of mass, momentum, energy within jet or mixing layers and apparent increasing in ejector performance concerned to MOC_SHORT nozzle contour is governed by the turbulence properties at the nozzle exit plane for sure. However, steady RANS approach coupled with two-equation turbulence model is incapable to capture such sophisticated features of compressible turbulent flows. The fact of ejector's performance gain with MOC_SHORT nozzle contour is connected to the smallest boundary layer momentum thickness (fig. 4b) as well as to maximum mass fraction of the liquid phase at the nozzle exit lip. These two factors in sum increase the momentum of the motive flow in the mixing layer thereby causing the secondary mass flow rate augmentation.

4. Conclusions

The present CFD study revealed that the shortest nozzle contour designed by the axisymmetric Method of Characteristic and accompanied with the maximum expansion rate of the flowfield (MOC_SHORT) results in better overall steam ejector performance. Such outcome is not evident by relying on solely primary nozzle analysis or utilizing "dry" flow solution. The fact that only wet steam modeling comprises the full ejector domain can yields the most accurate results. Although, the nozzle contour possessing the better performance is found out, an additional research that would have included overexpanded flow modes with different levels of steam superheating is required to estimate all the factors properly. Besides, employing LES/DES treatment instead of steady RANS can shed light on turbulence quantities that are responsible for the secondary mass flow rate augmentation within mixing layer.

References

- [1] Mazzelli F., Giacomelli F., Milazzo A. 2018. CFD modeling of condensing steam ejectors: Comparison with an experimental test-case *International Journal of Thermal Sciences* 127 pp 7-18
- [2] Ariaifar K., Buttsworth D., Al-Doori G. 2015. Effect of mixing on the performance of wet steam ejectors *Energy* 93 pp 2030–2041
- [3] Al-Doori G. 2013. Investigation of refrigeration system steam ejector performance through experiments and computational simulations *Dissertation*
- [4] Starzmann J. et al. 2016. Results of the international wet steam modeling project *Proceedings of Wet Steam Conference* Prague
- [5] James E.J and Theo G.K. 2006. Gas Dynamics (third edition) Pearson Education New Jersey
- [6] Edathol J., Brezgin D., Aronson K., Kim H.D. 2020. Prediction of non-equilibrium homogeneous condensation in supersonic nozzle flows using Eulerian-Eulerian models *International journal of heat and mass transfer* 152
- [7] Lamanna G. 2000. On Nucleation and Droplet Growth in Condensing Nozzle Flows *Dissertation* Technische Universität Eindhoven
- [8] Menter F.R., Lechner R., Matsyushenko A. 2019. Best Practice: Generalized k- ω Two-Equation Turbulence Model in ANSYS CFD (GEKO)
- [9] Wilcox D.C. 2007. Formulation of the k- ω Turbulence Model Revisited. AIAA Paper p 1408
- [10] Herwig. H, Kock F. 2006. Direct and indirect methods of calculating entropy generation rates in turbulent convective heat transfer problems. *Heat and Mass Transfer* 43 pp 207-215
- [11] Starzmann J et al. 2016. Numerical investigation of boundary layers in wet steam nozzles. *Proceedings of ASME Turbo Expo 2016* Seoul, South Korea
- [12] Zucrow M.J and Hoffman J.D. 1976. Gas Dynamics v.1 John Wiley & Sons, INC